Location of Ion-Acoustic Waves from Back and Side Stimulated Brillouin Scattering

C. Labaune, H. A. Baldis, E. Schifano, B. S. Bauer,* A. Michard, and N. Renard
Laboratoire pour l'Utilisation des Lasers Intenses, Ecole Polytechnique, France

W. Seka
Laboratory for Laser Energetics, University of Rochester, Rochester, New York 14627

J. D. Moody and K. G. Estabrook
Lawrence Livermore National Laboratory, Livermore, California 94550
(Received 13 February 1996)

Direct observation of the location of ion-acoustic waves (IAWs) explains for the first time the stimulated Brillouin scattering (SBS) spectra in backward and side directions. The regions of SBS activity are limited and smaller than the scale length of the plasma. The IAWs are localized in the front part of the plasma, resulting in blue Doppler shift of the scattered electromagnetic wave, and the distance from the summit changes with the SBS angle. [S0031-9007(96)00210-4]

PACS numbers: 52.35.Fp, 52.35.Nx, 52.40.Nk, 52.50.Jm

Stimulated Brillouin scattering (SBS) [1] is an important instability in the context of inertial confinement fusion (ICF), which has been studied up to now mainly from the electromagnetic wave (EM) associated with the decay, and primarily in the backward direction [2]. Sidescattering can strongly affect the redistribution of laser energy in both direct and indirect drive [3], modifying the initial energy balance between the beams. This is particularly true in the case of indirect drive where direct irradiation of the capsule is to be avoided, and where sidescattering can contribute to coupling between beams at the crossing points [4].

Stimulated Brillouin scattering consists of the decay of the incident EM wave$(\omega_0, \vec{k}_0)$ into a scattered EM wave $(\omega_{\mathrm{SBS}}, \vec{k}_{\mathrm{SBS}})$ and an ion-acoustic wave (IAW) $(\omega_{\mathrm{IAW}}, \vec{k}_{\mathrm{IAW}})$ where ω and k are the frequency and wave number, respectively, for each wave. The scattering geometry is defined by the direction of propagation of the scattered EM wave. We define θ as the angle between the scattered EM wave and the pump EM wave ($\theta = 180°$ is direct backscatter). Of the two waves produced in the decay, only the IAW can provide information about the location and the extent of the region of activity. Information on the IAW can be obtained by Thomson scattering of a short wavelength probe beam [5]. This technique provides the most direct characterization of these waves, including their frequency, wave number, and location. Evidence of stimulated Brillouin sidescattering has been obtained in the past from the EM scattered light of wavelength near the incident laser [6], but information coming from these waves is limited because they are integrated along the direction of propagation, and refraction of the scattered light can significantly change the angular distribution of the scattered light [7].

This paper presents the first data on the localization of IAWs and their correlation with the EM waves from the same SBS decay for side and backward directions. The measurement of the location of IAWs in the density profile provides the required Doppler shift correction of the scattered EM waves, which are then in good agreement with the observed SBS spectra. Blueshifts and redshifts of backward and side scattering, respectively, can be explained by the change of location of the associated IAWs, confirming the assumptions made in many past experiments [8]. A novelty of this experiment is the use of three different interaction beams, with the same characteristics, to irradiate a well-characterized preformed plasma. This multiple beam configuration allowed the study of IAW over a large range of scattering angles, using the same Thomson scattering probe and collecting optics, and the same SBS station. Using one beam at the time and the same SBS station provided exact measurements of SBS as a function of the angle, eliminating uncertainties due to calibration of separate diagnostics.

The experiments described in this paper have been performed using the six beams of the Laboratoire pour l'Utilisation des Lasers Intenses (LULI) laser facility. The geometry of the configuration is shown in Fig. 1. The pulse shape of all beams was Gaussian with a full width at half maximum (FWHM) of 0.6 ns. The timing and characteristics of the beams were as follows. The plasma was formed by two opposite beams (A and E in Fig. 1) with a wavelength of 526 nm and maximum at $t = 0$. The three interaction beams (C, F, and D in Fig. 1) have a wavelength of 1.053 μm and a timing of $t = 1.72$ ns after the plasma producing beams. Each of these beams was focused with an $f/6$ lens combined with an RPP of 2 mm elements. This produced a focal spot with 64% of the energy into a 320 μm diameter spot, with a maximum intensity of 10^{14} W/cm^2. The probe beam (B) started 240 ps before the interaction beam in order to probe the

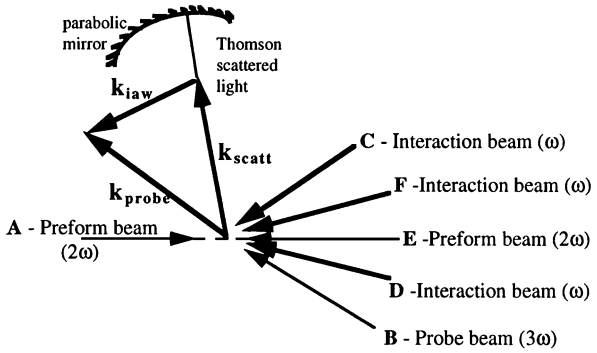

FIG. 1. Configuration of the laser beams and geometry of Thomson scattering.

interaction at the very early stage, and had a wavelength of 351 nm. It was focused with an $f/2.5$ lens and an RPP with elongated elements, 0.1×0.9 mm, producing a line focus of 100 μm $\times$ 1 mm along the axis of the interaction beam.

The targets were small disks of $(CH)_n$, 1.5 μm thick. The diameter of 400 μm was chosen to be smaller than the focal spot diameter of the plasma producing beams. The advantage of using mass limited targets is that there is no matter left when the probe beam arrives, so eliminating any possible parasitic scattered light. They were placed normal to the interaction beam under use, in order to have the plasma expansion along the axis of the beam. At the time of interaction, the plasma had a density profile with an approximately inverse parabolic shape along the laser direction with a scale length of $\sim$1 mm and was flat over a distance of 400 μm in the transverse direction. The maximum electron density evolved from 25% to 8% of critical density ($n_c = 1.1 \times 10^{21}$ cm^{-3} is the critical electron density for $\lambda_0 = 1.05$ μm light) during the interaction pulse, with an electron temperature of 0.5 keV [9].

The Thomson scattering was set up to probe the IAWs associated with SBS. The plasma was imaged onto the slits of an array of spectrometers and streak cameras to obtain time, space, and frequency resolved density fluctuations associated with the IAWs. The frequency and wave number of the Thomson scattered light are given by $\omega_{\text{scatt}} = \omega_{\text{probe}} - \omega_{\text{IAW}}$, $\vec{k}_{\text{scatt}} = \vec{k}_{\text{probe}} - \vec{k}_{\text{IAW}}$. The probed IAWs correspond to different angles of SBS scattering (θ), depending on the choice of interaction beam. Figure 2 shows the general wave vector diagrams for the SBS decay of each of the interaction beams. The Thomson scattered light with angles between 15 and 49° from the probe axis, was collected by an off-axis parabolic mirror. These angles cover a range of SBS angles $\theta = 150°–180°$ for beam F, of $\theta = 130°–160°$ for beam C, and $\theta = 70°–100°$ for beam D. Improved angular resolution was obtained by using vertical masks on the scattered light beam, limiting the collecting angle to 5°. The SBS diagnostic analyzed light collected by the focusing lens of beam F ($\delta\Omega = 0.045$ sr). This provides the time-resolved spectra and reflectivity measurements for backscattering, sidescattering at $\theta = 157,5°$ and at $\theta = 135°$ for interaction beams F, C, and D, respectively.

Figure 3 shows the location of ion-acoustic fluctuations associated with three SBS angles ($\theta = 180, 157, 5$, and 135°) as a function of time. The range of wavelengths shown in this figure was selected using color and interference filters, with a bandpass of 150 Å centered at 351 nm. As a function of time, two signals are observed in each of these frames. The first signal is the three-halves harmonic produced by the interaction of the plasma producing beams with the plasma ($3/2 \times 2\omega = 3\omega$). This emission is not isotropic and, due to the scattering geometry, the predominant contribution is from beam E. This signal provides good spatial and temporal references for the different images. The second signal is the Thomson scattered light from the IAWs associated with SBS during the interaction pulse.

As can be clearly seen from Fig. 3, the density fluctuations are larger for backscattering than for sidescattering. Assuming that the scattering is from a coherent ion acoustic wave, the Thomson scattered power (P_{scatt}) is proportional to the square of the density fluctuation level (δ_n/n) associated to the IAWs and to the power of the probe beam (P_{probe}). The relation can be written [10]: $P_{\text{scatt}} = \frac{1}{4}(\delta n/n)^2 P_{\text{probe}} A r_e^2 n_e^2 \lambda_{\text{probe}}^2 L_z^2$, where A is a geometrical factor which takes into account the imaging of the plasma onto the slit of the streak camera, r_e is the classical radius of the electron, n_e is the electron density, λ_{probe} is the wavelength of the probe beam, and L_z is the length of the interaction region along the probe axis. We used the Bremsstrahlung emission of the plasma, between 380 and 390 nm, to calibrate the system. The measured scattered power corresponds to an average density fluctuation level of $\sim 5 \times 10^{-4}$ for the IAWs associated to

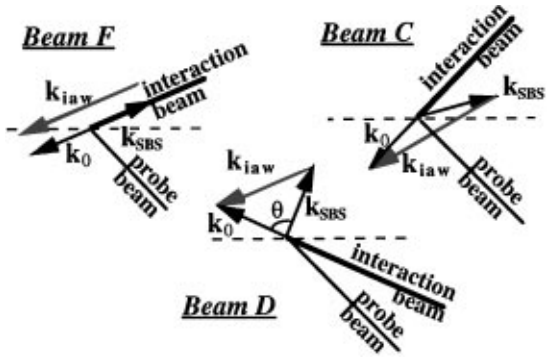

FIG. 2. Wave-vector diagrams for the SBS decay of each of the interaction beams. The ion-acoustic waves which can be probed by the Thomson scattering diagnostic correspond to SBS angles $\theta = 150°–180°$ for beam F, $\theta = 130°–160°$ for beam C, and $\theta = 70°–100°$ for beam D.

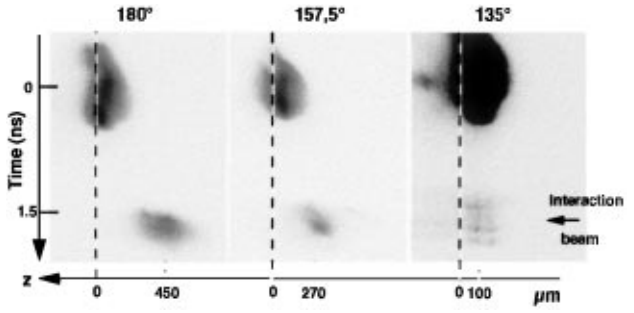

FIG. 3. Location of the ion-acoustic waves associated to SBS for different SBS decompositions: 180, 157,5, and 135° with respect to the pump beam. The interaction beam is coming from the right. The initial target position, or top of the density profile, is at $z = 0$. The early signal corresponds to plasma emission during preforming beams, and time $t = 0$ refers to the maximum of these beams. The late signal corresponds to Thomson scattered light from IAWs during the interaction.

backscattered SBS. The variations of density fluctuations with the SBS decay angle agree with the observed variations on the SBS reflectivities as a function of angle, shown in Fig. 4. The SBS reflectivity in backscattering direction is a few percent, with a fast decrease as a function of the SBS angle: by a factor of ~80 for 157,5° and $\sim 10^3$ for 135° compared to backscattering.

A new and important result is the localization of ion-acoustic fluctuations in a small region of the density profile in the front part of the plasma relative to the interaction beam region that changes with the SBS decay geometry. In all cases, the interaction region is smaller than the scale length of the plasma. The duration of the Thomson scattered signal has a full width at half maximum of ~300 ps, shorter than the interaction pulse, with its maximum at ~150 ps before the maximum of the interaction pulse.

The temporal behavior of the ion-acoustic fluctuations can be explained [11] by the evolution of the SBS gain using linear theory. The SBS gain depends mainly on five parameters which are the laser intensity, electron density and electron temperature, density, and velocity gradient scale lengths [12,14]. The temporal increase of the SBS gain follows the laser intensity, while the drop of the SBS gain is due to a combination of reduction of the electron density due to plasma expansion and increase of temperature due to plasma heating by the interaction beam.

The spatial behavior of SBS is new and cannot be predicted by the linear theory applied to the averaged intensity and reflectivity. The two parameters which can produce spatial variation of the gain along the laser axis, in the Rosenbluth formula, are the laser intensity and the flow velocity. We found that, even if we include inverse Bremsstrahlung absorption, SBS losses, and change of direction of the flow velocity for the two sides of the plasma, the gain is still maximum close to the summit of the density profile. Location of SBS in the front part of the plasma has been observed in numerical simulations [13], due to a higher laser intensity in this region because of the beating of the incident and backscattered waves, as well as pump depletion due to high SBS reflectivities. This does not apply to the overall beam in our experiment, as the averaged SBS reflectivity for backscattering is only a few percent and overall pump depletion is not significant.

A realistic interpretation of these results can be done by considering the real intensity distribution in the focal volume as produced by the random phase plate and applying the theory of Brillouin in the statistics of speckles rather than to the average laser intensity [15]. Then stimulated scattering from some high intensity speckles could be very strong, with nonlinear processes being involved, but the number of statistically significant speckles in the interaction volume can be relatively small and have a minor effect on the overall beam propagation through the plasma. Such speckles are in the regime of strong pump depletion, leading to a shift of the maximum intensity from the center of the speckle towards the laser, and similarly for the maximum of density perturbations. This description of SBS in an individual speckle is then averaged over the statistical distribution of speckles in the plasma, and the observed density fluctuations exhibit the same shift towards the laser. This theory cannot account, nevertheless, for the change of location of the ion acoustic

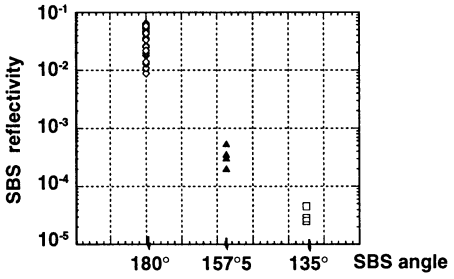

FIG. 4. Angular distribution of stimulated Brillouin scattering reflectivity.

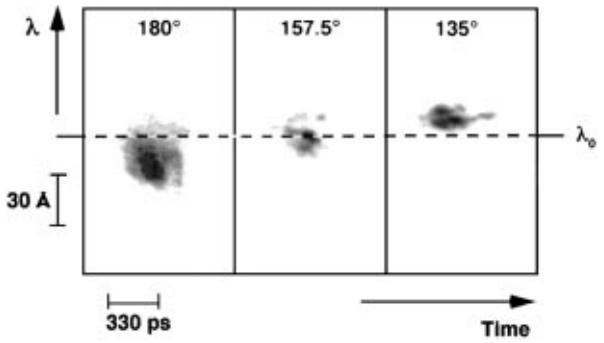

FIG. 5. Time-resolved spectra of scattered light at three rearward angles: 180, 157,5, and 135°.

waves with the SBS angle. A possible explanation for this discrepancy is that the dominant process of backward SBS suppresses much weaker processes of side scattering, because of nonlinear damping or detuning for other ion acoustic waves [16].

The time-resolved spectra of the scattered light by the SBS instability are shown in Fig. 5 for the same three angles of decay as in Fig. 3. The spectrum is wide and completely blueshifted in the case of backscatter. They are narrower, and nonshifted or redshifted for 157,5 and 135°, respectively. Using the locations of the IAWs associated with each SBS decay measured in the experiment and the velocity profile from LASNEX simulations, we have calculated the shift of the SBS spectra produced by both the Brillouin and the Doppler effects: $\delta\lambda(\text{Å}) = (\lambda^2/2\pi c)k_{\text{IAW}}[c_s - u\,\sin(\theta/2)]$, where c_s is the sound speed and u is the expansion velocity $[u(\text{cm/s}) = 6 \times 10^4 z(\mu\text{m})]$. For our conditions the shift is given by

$$\delta\lambda(\text{Å}) = 7.02(1 - n_e/n_c)^{1/2}\sin(\theta/2) \times [2.27T_e^{1/2}(\text{keV}) - 6\times 10^{-3} z(\mu\text{m})\,\sin(\theta/2)].$$

For IAWs positions between 200 and 600 μm, and backscatter geometry, this formula predicts spectral shifts between -15 and $+2$ Å from the laser wavelength. For positions between 190 and 400 μm, and $\theta = 157°$, this formula predicts spectral shifts between -5 and $+3$ Å from the laser wavelength. For positions between 0 and 200 μm, and $\theta = 130°$, this formula predicts spectral shifts between 3 and 10 Å from the laser wavelength. These calculated spectral shifts agree well with the observed SBS spectra. The measured SBS spectra are a little wider than the calculated ones. This difference can be explained by the fact that the volume of plasma which contributes to the SBS light may be larger in the transverse direction than the one which is probed along the laser axis by the Thomson scattering diagnostic.

In conclusion, we have observed good correlation between the location of ion-acoustic waves and the spectra of electromagnetic waves generated in the same stimulated Brillouin scattering decay, in backward and in side directions. Furthermore, these results are the first direct observation of the growth of the IAWs in the front part of the density profile. These new observations prove speculations made in many past experiments that have shown blueshifted backward SBS. The observed change of location of IAWs with the SBS angle confirms previous speculations, that scattering at each SBS angle originates at a different location in the plasma, proposed to explain side SBS spectral shifts [17].

We are thankful for the support of all the technical groups of LULI who provided important optical, mechanical, and electronic assistance. We gratefully acknowledge useful discussions with V. Tikhonchuk and G. Laval. Part of this work was performed under the auspices of the U.S. Department of Energy by the Lawrence Livermore National Laboratory under Contract No. W-7450-Eng-48.

*Present address: Department of Physics, University of Nevada, Reno, NV 89557.

[1] W. L. Kruer, *The Physics of Laser Plasma Interactions* (Addison-Wesley Publishing Company, Redwood City, California, 1988).
[2] H. A. Baldis, E. M. Campbell, and W. L. Kruer, in *Physics of Laser Plasmas*, edited by A. Rubenchik, W. Witkowski (North-Holland, Amsterdam, 1991), pp. 361–434.
[3] J. Lindl, Phys. Plasmas **2**, 3933 (1995).
[4] W. L. Kruer, S. C. Wilks, B. B. Afayan, and R. K. Kirkwood, Phys. Plasmas **3**, 1 (1996); V. V. Eliseev, W. Rozmus, V. T. Tikhonchuk, and C. E. Capjack (to be published).
[5] H. A. Baldis, D. M. Villeneuve, and C. J. Walsh, Can. J. Phys. **64**, 961 (1986).
[6] R. A. Haas *et al.*, Phys. Fluids **20**, 322 (1977); B. H. Ripin, Appl. Phys. Lett. **30**, 134 (1977); K. Tanaka and L. M. Goldman, Phys. Rev. Lett. **45**, 1558 (1980).
[7] P. E. Young and K. G. Estabrook, Phys. Rev. E **49**, 5556 (1994).
[8] A. N. Mostovych *et al.*, Phys. Rev. Lett. **59**, 1193 (1987); K. Tanaka *et al.*, Phys. Fluids **27**, 2960 (1984); D. Phillion *et al.*, Phys. Rev. Lett. **39**, 1529 (1977); M. D. Rosen *et al.*, Phys. Fluids **22**, 2020 (1979); P. E. Young *et al.*, Phys. Fluids B **2**, 1907 (1990); P. E. Young, H. A. Baldis and K. G. Estabrook, Phys. Fluids B **3**, 1245 (1991); A. V. Chirokikh, W. Seka, R. S. Craxton, R. E. Bahr, A. Simon, R. W. Short, E. M. Epperlein, H. A. Baldis, and R. P. Drake, Bull. Am. Phys. Soc. **38**, 1934 (1993).
[9] C. Labaune *et al.*, Phys. Rev. Lett. **75**, 248 (1995).
[10] R. E. Slusher and C. M. Surko, Phys. Fluids **23**, 472 (1980).
[11] C. Labaune *et al.*, "Interplay between Electron Plasma Waves and Ion-Acoustic Waves in a Laser-Produced Plasma" (to be published).
[12] D. W. Forslund, J. M. Kindel, and E. L. Lindman, Phys. Fluids **18**, 1002 (1975).
[13] S. Huller, *et al.* (to be published); M. R. Amin *et al.*, Phys. Fluids B **5**, 3748 (1993).
[14] C. S. Liu, M. N. Rosenbluth, and R. B. White, Phys. Fluids **17**, 1211 (1974).
[15] V. Tikhonchuk, C. Labaune, and H. A. Baldis, "Analysis of a Stimulated Brillouin Scattering Experiment with Statistical Distribution of Speckles" (to be published).
[16] A. V. Maximov, W. Rosmus, D. F. Dubois, H. A. Rose, A. M. Rubenchik, V. T. Tikhonchuk, Phys. Plasmas **3**, 198 (1996).
[17] S. H. Batha *et al.*, Phys. Rev. Lett. **70**, 802 (1993).